

平面光波導元件之鉕共摻雜氧化鈦基薄膜材料製程與光電特性研究

Physical characteristics and optical properties of sol-gel derived Er³⁺-Yb³⁺ codoped TiO₂ for optical waveguide

計畫編號：NSC90-2216-E-009-041

執行時間：90/08/01 ~ 91/07/31

主持人：陳三元 副教授

交通大學材料科學與工程系

中文摘要

本研究主要是在探討氧化鈦材料來當作母材的鉕、釔共摻雜氧化鈦薄膜，其藉由釔離子的共摻雜，將使得此薄膜所放射出的~1.54 μm 螢光的發光強度較現今被廣泛報導且具有良好螢光特性的鉕、鋁共摻雜氧化矽薄膜的螢光強度還強約 17 倍，且此螢光頻譜的半高寬亦增寬約 1.4 倍，此外，同時此薄膜亦具有較低的製程溫度(比鉕、釔共摻雜氧化矽之製程溫度低~300°C)，故其可應用在積體光學中平面光波導放大器的製作上。

關鍵詞：鉕、釔共摻雜氧化鈦、螢光、溶凝膠、分散性

Abstract

Er³⁺-Yb³⁺ codoped TiO₂ films were prepared on fused silica by sol-gel processes. The maximum ~1.54 μm photoluminescence (PL) intensity occurs in the Er³⁺ (5 mol %)-Yb³⁺(30 mol %) codoped TiO₂ samples annealed at 700 °C. However, when the concentration of Yb³⁺ ions attends to 50 mol %, the back energy transfer effect from Er³⁺ to Yb³⁺ will deteriorate the ~1.54 μm PL efficiency. It was believed that the Yb³⁺ ion does not only play a disperser but also a sensitizer to Er³⁺ ion. This dual effects lead to the larger PL intensity in Er³⁺-Yb³⁺ codoped TiO₂ system than that in Er³⁺-Y³⁺ codoped TiO₂ system. Even compared with the SiO₂ films with Er³⁺ (3 mol %)-Yb³⁺ (30 mol %) codoped and annealed at an optimal temperature of 985 °C, the Er³⁺-Yb³⁺ codoped TiO₂ film can obtain better PL properties at a lower annealing temperature.

Key words: Er³⁺-Yb³⁺ codoped TiO₂ 、 photoluminescence 、 sol-gel 、 dispersion

1. Introduction

TiO₂ film has higher refraction index (n=2.52 for anatase and n=2.76 for rutile) as well as lower phonon energy (<700 cm⁻¹)¹ than silica glass film, Er³⁺-doped TiO₂-based films have shown potential applications in the micro-integrated photonic devices. However, little detailed studies were made

to investigate the role of Er³⁺ content in the PL properties of Er³⁺-doped TiO₂ films.^{2,3}

The Yb³⁺ codopant has been demonstrated in increasing the variation of Er sites that results in the inhomogeneous broadening effect.⁴ In addition, Yb³⁺ ion can sensitize Er³⁺ ions so as to enhance the ~1.54 μm PL intensity.⁵ However, the role of Yb³⁺ ion in phase development and related optical properties of Er³⁺-doped TiO₂ system has been not investigated. Furthermore, Yb³⁺/Y³⁺/Er³⁺ ions have similar ionic radii (Yb³⁺ = 0.0862, Y³⁺ = 0.0892, and Er³⁺ = 0.0881 nm) and Yb₂O₃/Y₂O₃/Er₂O₃ have nearly the same crystal structural and lattice constant.

Therefore, it is very important to investigate the influence of co-dopant Yb³⁺ on the physical characteristics and optical properties of Er³⁺-doped titania. Furthermore, the role of Yb³⁺ and Y³⁺ codopants in photoluminescence properties of Er³⁺-doped titania materials will be discussed and compared.

2. Experimental

A. Thin films preparation

The Er³⁺-Yb³⁺ codoped TiO₂ films were prepared from yttrium acetate, erbium acetate (Alfa) and titanium isopropoxide. The as-deposited films were first pyrolyzed under dry oxygen atmospheres at 400 °C for 30 min and then annealed at 600-1000 °C for 1 h in dry oxygen atmosphere.

B. Characterization measurements

The phase structures of films were analyzed by X-ray diffractometer. The electron spin resonance (ESR) spectra were recorded using a Bruker ESR spectrometer. The fluorescence spectra were excited by a 980 nm diode laser. Erbium L_{III}-edge X-ray absorption spectra were recorded at Synchrotron Radiation Research Center (SRRC), Hsinchu.

3. Results and discussion

3.1. Structural evolution

The X-ray diffraction (XRD) patterns in Fig. 1(a) show the effect of annealing temperatures on structural evolution of Er³⁺ (5 mol %)-doped TiO₂. It is obvious that the addition of more than 5 mol %

Er^{3+} ions can lead to the destruction of TiO_2 network structure. The crystallinity of anatase TiO_2 was reduced and anatase-to-rutile (A \rightarrow R) transformation rate was accelerated (e.g., the anatase phase totally disappear at 900 °C annealing). Additionally, the $\text{Er}_2\text{Ti}_2\text{O}_7$ pyrochlore phase (P) was detected at 800 °C. For the Er^{3+} (5 mol %)- Yb^{3+} (30 mol %) codoped TiO_2 samples, the XRD patterns in Fig. 1(b) show that when the samples were annealed 700 °C, the host matrix becomes amorphous for Yb^{3+} concentration above 10 mol %. Additionally, Yb^{3+} codopant was found to accelerate the A \rightarrow R transformation; all of the anatase phase has been transformed into rutile phase at 800 °C. After the Er^{3+} - Yb^{3+} codoped TiO_2 samples were annealed at 900-1000 °C, both rutile (R) and pyrochlore (P) phase become more well-crystallized. Similar results are also observed in the Y^{3+} -doped TiO_2 system.

In addition, Fig. 2 shows the surface morphologies of Er^{3+} -doped TiO_2 and Er^{3+} - Yb^{3+} codoped TiO_2 samples annealed 700°C/1 h. The grain sizes of the TiO_2 samples doped with Er^{3+} (5 mol %), Er^{3+} - Yb^{3+} (5-10 mol %) are about 60 and 25 nm, respectively. It has been well known that smaller grains can provide more surface nucleation sites, which can accelerate the A \rightarrow R phase transformation. Therefore, the smaller grain size in Er^{3+} - Yb^{3+} codoped TiO_2 samples than Er^{3+} -doped TiO_2 samples reflects the higher A \rightarrow R transformation rate.

Figure 3 shows the pseudo-radial distribution functions obtained from the k^3 -weighted Fourier transforms of the Er^{3+} - Yb^{3+} codoped TiO_2 samples annealed at 700 for 1 h. Qualitative observation of the 700°C-annealed samples (i.e., no formation of pyrochlore phase) reveals that the first and second-neighbor distance around Er^{3+} is close to the Er-O and Er-Er bond length of Er_2O_3 , respectively. This means that the local structure around Er^{3+} ions in the Er^{3+} - Yb^{3+} codoped TiO_2 systems is similar to that of the crystalline Er_2O_3 . Additionally, it is noted that the second-neighbor distance around Er^{3+} slightly increased with the increase of Yb^{3+} concentration up to 30 mol%. The increased second-neighbor distance seems to reveal that the second shell may partially contain Yb^{3+} ions. This phenomenon can be attributed to the fact that as Er^{3+} and Yb^{3+} have the same valence and close ionic radii, they can be replaced with each other. However, as the Er^{3+} -doped TiO_2 was codoped with 50 mol% Yb^{3+} , the second-neighbor distance around Er^{3+} becomes larger as compared to that with 30 mol% Yb^{3+} codoped that is probably due to a high disorder around Er^{3+} ions.

3.2. $\sim 1.54 \mu\text{m}$ photoluminescence properties

Figure 4 shows the $\sim 1.54 \mu\text{m}$ PL spectra of the Er^{3+} (5 mol %)-doped TiO_2 samples with 0-50 mol % Yb^{3+} added and annealed at 700 °C for 1 h. All of the spectra were normalized to the same intensity to compare the difference between spectral features. The Er^{3+} (5 mol %)-doped TiO_2 sample exhibits a sharp PL spectrum with a $1.537 \mu\text{m}$ main peak which is characteristic emission (${}^4I_{13/2} \rightarrow {}^4I_{15/2}$) of Er^{3+} ion. However, by increasing the Yb^{3+} codopant concentration, the PL spectra became more broaden. The maximum bandwidth (FWHM= 67 nm) of $\sim 1.54 \mu\text{m}$ PL spectra was obtained for the sample added with Yb^{3+} content above 30 mol %. The line-broadening mechanism can be attributed to the inhomogeneously broadened transition of Er^{3+} ions.⁶ For the sample without Yb^{3+} codopant, the well-resolved spectrum demonstrates that the Er^{3+} ions are located in well-defined sites of TiO_2 matrix. Namely, each Er^{3+} ion occupies the similar type of site that has well-defined surrounding and hence each Er^{3+} ion experiences the similar crystal field. However, the Yb^{3+} codopant can destroy the network of TiO_2 host matrix, which results in the varying Er sites with different surrounding environment and causes a randomization of the Stark splittings. Therefore, the overall spectral lines resulting from the superimposed contributions of each Er site are inhomogeneously broadened.

Figure 5 illustrates that the influence of annealing temperatures on the $\sim 1.54 \mu\text{m}$ PL spectral feature of Er^{3+} (5 mol%)- Yb^{3+} (30 mol%) codoped TiO_2 samples. The higher annealing temperature (≥ 800 °C) leads to the spectra with many splitting lines. From the XRD detection, it shows that the $\text{Er}_2\text{Yb}_{2-x}\text{Ti}_2\text{O}_7$ crystallites were generated at the annealing temperatures above 800 °C. This means that the majority of Er^{3+} ions should be located in the crystalline $\text{Er}_2\text{Yb}_{2-x}\text{Ti}_2\text{O}_7$ phase and the Er^{3+} bonding environment becomes uniform to produce the well-resolved PL spectrum.

The variation of the $\sim 1.54 \mu\text{m}$ PL intensity of Er^{3+} - Yb^{3+} codoped TiO_2 samples with Er^{3+} - Yb^{3+} concentration was summarized in Fig. 6. By codoping 10-30 mol % Yb^{3+} ions into Er^{3+} -doped TiO_2 samples, the PL intensity can be remarkably enhanced. Nevertheless, the 50 mol % Yb^{3+} codopant leads to the reduction of PL intensities that might be related to the back energy transfer from Er^{3+} to Yb^{3+} ions⁶ and the double energy transfer (DET). For comparison, the Er^{3+} (5 mol%)- Yb^{3+} (30 mol%) codoped silica film was also prepared and annealed at an optimal temperature of ~ 985 °C. Figure 7 illustrates that the PL properties of the Er^{3+} - Yb^{3+} codoped TiO_2 system exhibit more intense emission (~ 2 times) and wider FWHM

(~1.5 times) than those of optimal $\text{Er}^{3+}\text{-Yb}^{3+}$ codoped SiO_2 system. This result implies that the PL properties strongly depend on the composition and structure of the host materials. Furthermore, the $\text{Er}^{3+}\text{-Yb}^{3+}$ codoped TiO_2 film does not only obtain better PL properties but also lower annealing temperature.

The dependence of annealing temperatures on the PL intensities of Er^{3+} (5 mol %)- Yb^{3+} (30 mol %) codoped TiO_2 samples were shown in Fig. 8. The increase in PL intensity from 600 to 700 °C is attributed to the reduction of OH^- hydroxyl content (as one can see in Fig. 9, the decrease of FTIR absorption around 4000-3000 cm^{-1} corresponding to the O-H vibration mode increases with the annealing temperature.).⁷ However, above 800 °C, the PL intensity is abruptly reduced that is strongly related to the formation of pyrochlore phase. The $\text{Er}_x\text{Yb}_{2-x}\text{Ti}_2\text{O}_7$ pyrochlore crystallites as identified from XRD patterns are generated at 800 °C and its crystallinity can be enhanced at higher temperature annealing. Therefore, the local structure around Er^{3+} ions in the well-crystallized $\text{Er}_x\text{Yb}_{2-x}\text{Ti}_2\text{O}_7$ phase becomes higher-order symmetry compared to that of Er^{3+} ions in amorphous host matrix. That results in the reduced probability of the normally forbidden intra-4f transition of Er^{3+} ions and the degradation in the PL efficiency.⁸

On the other hand, for the Er^{3+} -doped TiO_2 sample codoped with Y^{3+} , the ~1.54 μm PL spectra (no shown here) exhibit the similar effects to the $\text{Er}^{3+}\text{-Yb}^{3+}$ codoped TiO_2 samples. An enhancement of PL intensities with increasing Y^{3+} content was observed for the Er^{3+} (5 mol %)- Y^{3+} (10-50 mol %) codoped TiO_2 samples as shown in Fig. 10. In contrast, a maximum PL intensity appears at the sample of Er^{3+} (5 mol %)- Yb^{3+} (30 mol %) codoped TiO_2 , above that, a reduced PL intensity was observed such as for the sample with 50 mol% Yb^{3+} . As comparing the PL intensities of TiO_2 samples codoped with Er^{3+} (5 mol %)- Yb^{3+} (30 mol %) with Er^{3+} (5 mol %)- Y^{3+} (30 mol %), it demonstrates that the PL intensity in the former is about ~ 2 times higher than that in the latter. According to the aforementioned experimental results, the mechanisms for the enhancement of PL intensity between Yb^{3+} and Y^{3+} codoping are somewhat different.

For the $\text{Er}^{3+}\text{-Y}^{3+}$ (or $\text{Er}^{3+}\text{-Yb}^{3+}$) codoped TiO_2 systems without the formation of pyrochlore phase (i.e., the annealing temperature ≤ 700 °C), the EXAFS analysis (see Fig. 3) shows that the local environment of Er sites is similar to Er_2O_3 in host matrix. We believe that the Er sites with Er_2O_3 -like environment are optically active centers as the case in the Er^{3+} -doped silicate glasses.⁹ Because Er^{3+}

and Yb^{3+} (or Y^{3+}) have the same valence and similar ionic radii, they could be replaced with each other and the -Er-O-Er-O-Er- bonding structures can be changed into -Er-O-[Yb (or Y^{3+})-O]_n-Er-. Therefore, the more Y^{3+} codopant results in the larger atomic spacing among Er^{3+} ions and the enhanced PL properties that can be attributed to the increased dispersion and solubility of Er^{3+} ions in $\text{Er}^{3+}\text{-Yb}^{3+}$ (or $\text{Er}^{3+}\text{-Y}^{3+}$) codoped TiO_2 systems. However, it is worthy to note that with increasing Yb^{3+} up to 30 mol%, the PL intensity was remarkably enhanced. It implies that the Yb^{3+} ion does not only play a disperser but also a sensitizer to Er^{3+} ion. This dual effects might have the superimposed impact to the ~1.54 μm PL efficiency, which seems consistent with our experimental results that the $\text{Er}^{3+}\text{-Yb}^{3+}$ (10-30 mol %) codoped TiO_2 samples have larger PL intensity than that of $\text{Er}^{3+}\text{-Y}^{3+}$ (10-30 mol %) codoped TiO_2 samples.

4. Conclusions

- (1) The maximum ~ 1.54 μm PL intensity was obtained for the Er^{3+} (5 mol %)- Yb^{3+} (30 mol %) codoped TiO_2 sample and annealed at 700 °C. This can be attributed to the competition between the content of hydroxyl groups and Er site symmetry. Below 700 °C, the content of hydroxyl groups plays an important role in PL intensity. On the other hand, above 700 °C, the formed pyrochlore phases in the $\text{Er}^{3+}\text{-Yb}^{3+}$ codoped TiO_2 systems can result in the degradation of ~1.54 μm PL efficiency and the formation of well-resolved spectral lines.
- (2) The local chemical environment of Er^{3+} ions in $\text{Er}^{3+}\text{-Yb}^{3+}$ codoped TiO_2 films is similar to that in Er_2O_3 and the average spatial distance between Er^{3+} ions is slightly increased due to the partial substitution of Yb^{3+} for Er^{3+} ions in the Er_2O_3 -like local structure. That indicates that Yb^{3+} ion can act as disperser to Er^{3+} ions and reduce the concentration quenching effect.
- (3) In comparison with the $\text{Er}^{3+}\text{-Y}^{3+}$ codoped TiO_2 samples, the Yb^{3+} ion in the $\text{Er}^{3+}\text{-Yb}^{3+}$ codoped TiO_2 samples does not only play a disperser but also a sensitizer to Er^{3+} ion. This dual effects lead to the larger PL intensity in $\text{Er}^{3+}\text{-Yb}^{3+}$ codoped TiO_2 system than that in $\text{Er}^{3+}\text{-Y}^{3+}$ codoped TiO_2 system. However, when the concentration of Yb^{3+} ions attends to 50 mol %, the back energy transfer effect from Er^{3+} to Yb^{3+} will deteriorate the ~1.54 μm PL efficiency.

Acknowledgments

This work was financially supported by the

References

1. C. Urlacher and J. Mugnier, *J. Raman Spectrosc.* **27**, 785 (1996).
2. A. Bahtat, M. Bouazaoui, M. Bahtat, and J. Mugnier, *Opt. Commun.* **111**, 55 (1994).
3. A. Bahtat, M. Bouderbala, M. Bahtat, M. Bouazaoui, J. Mugnier, and M. Druetta, *Thin Solid Films* **323**, 59 (1998).
4. C. C. Robinson and J.T. Fournier, *J. Phys. Chem. Solids* **31**, 895 (1970).
5. E. Cantelar and F. Cussó, *Appl. Phys. B* **69**, 29 (1999).
6. E. F. Artemev, *Sov. J. of Quant. Electr.* **11**, 1266 (1981).
7. R. F. Bartholomew, B.L. Butler, H.L. Hoover, and C.K. Wa, *J. Am. Ceram. Soc.* **63**, 481 (1980).
8. B.A. Block and B.W. Wessels, *Appl. Phys. Lett.* **65**, 25 (1994).
9. M. Marcus, D. Jacobson, A. Vredenberg, and G. Lamble, *J. Non-Cryst. Solids* **195**, 232 (1996).

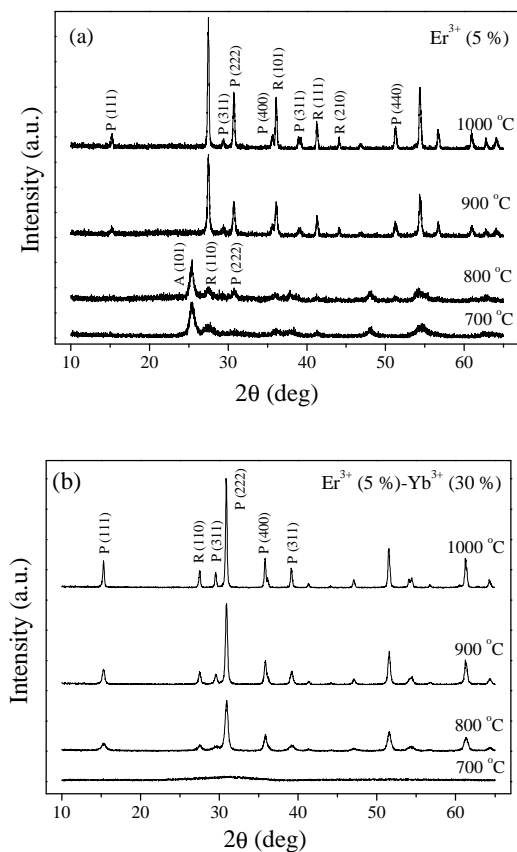


Fig. 1. XRD patterns of (a) Er^{3+} -doped TiO_2 and (b) different Er^{3+} - Yb^{3+} codoped TiO_2 films annealed at 700-1000 °C for 1 h.

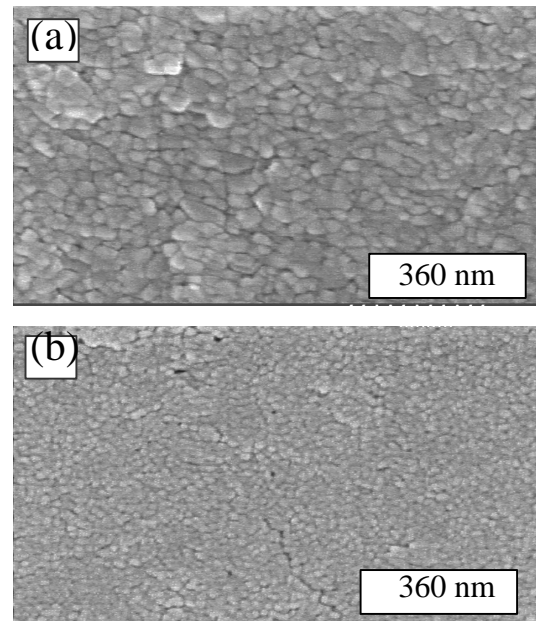


Fig. 2. Dependence of various Er^{3+} - Yb^{3+} codoped TiO_2 Films at 700 °C on refractive index.

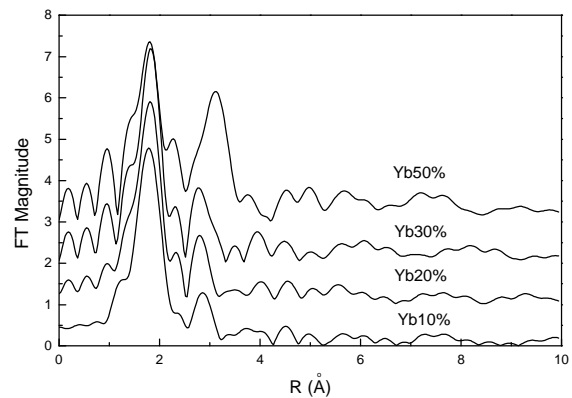


Fig. 3 Fourier transform of EXAFS function at Er L_{III} -edge for the samples annealed at 700 °C with various Yb content.

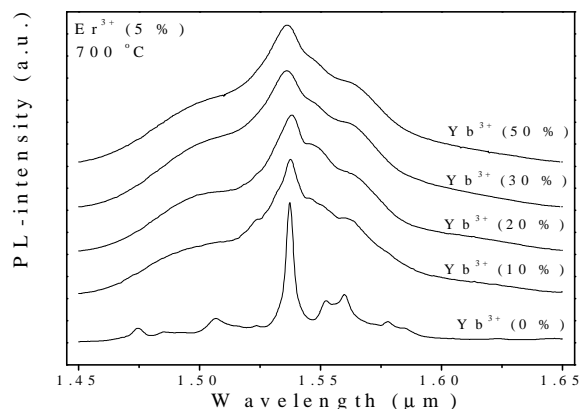


Fig.4 $\sim 1.54 \mu\text{m}$ PL spectra of the Er^{3+} (5 mol %) -doped TiO_2 samples with 0-50 mol % Yb^{3+} codopant annealed at 700 °C for 1 h.

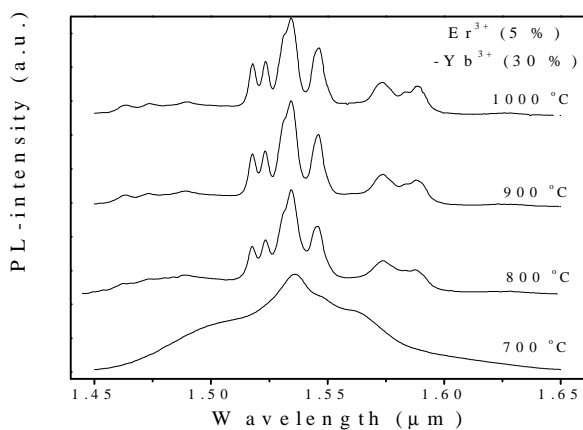


Fig. 5 $\sim 1.54 \mu\text{m}$ PL spectra of the Er^{3+} (5 mol %)- Yb^{3+} (30 mol %) codoped TiO_2 annealed from 700 to 1000 °C for 1 h.

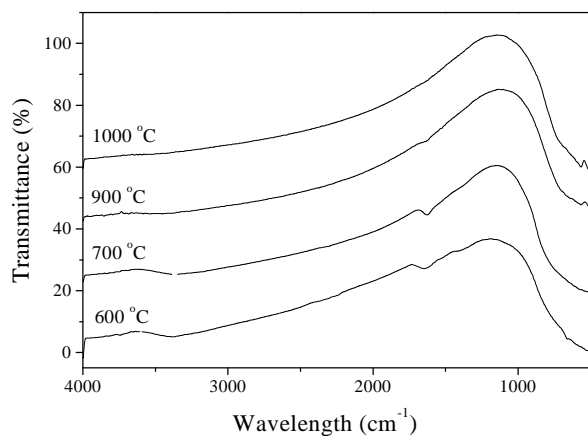


Fig. 8 Comparison of $\sim 1.54 \mu\text{m}$ PL spectra of Er^{3+} (5 mol %)- Yb^{3+} (30 mol %) codoped TiO_2 and SiO_2 films.

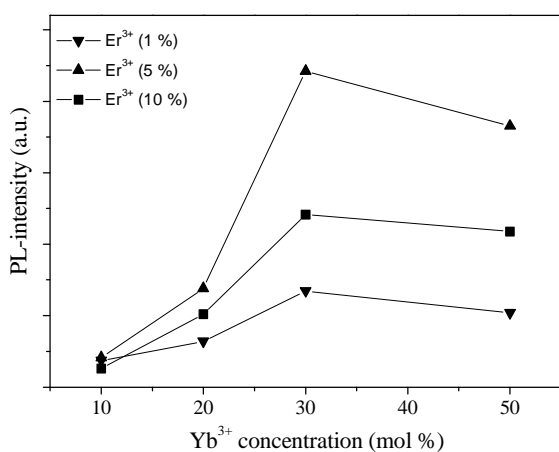


Fig. 6. Dependence of Yb^{3+} concentration on the $\sim 1.54 \mu\text{m}$ PL intensity of Er^{3+} - Yb^{3+} codoped TiO_2 samples added with different concentration of Er^{3+} ions and annealed at 700 °C/1 h.

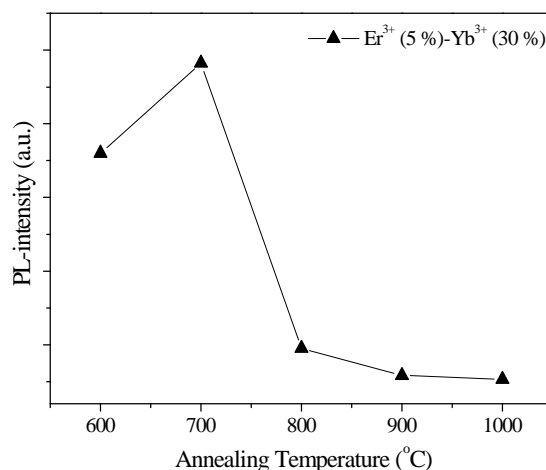


Fig. 9. FTIR transmittance spectra of Er^{3+} (5 mol %)- Yb^{3+} (30 mol %) codoped TiO_2 annealed from 600-1000 °C.

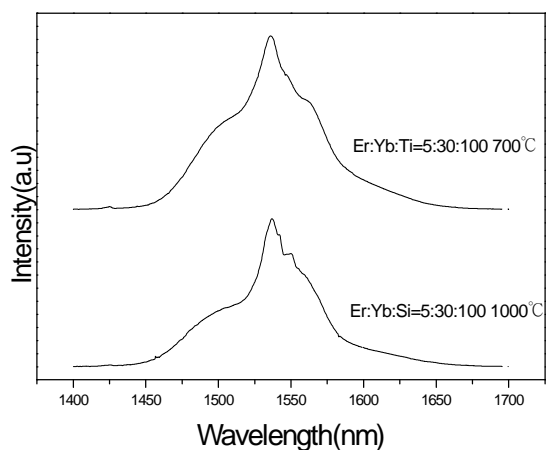


Fig. 7 PL intensity of the Er^{3+} (5 mol %)-doped TiO_2 samples with the 30 mol % Yb^{3+} codopant annealed from 600 to 1000 °C for 1 h.

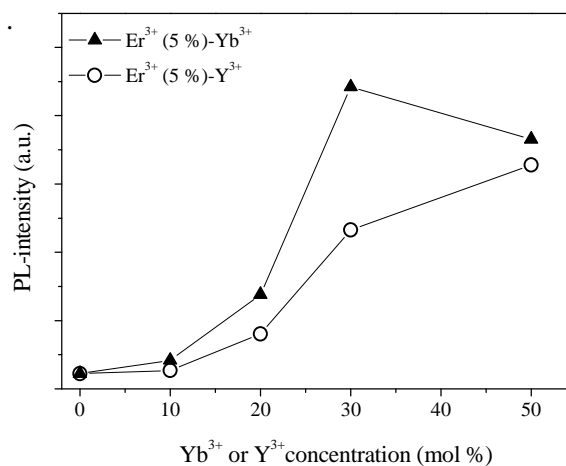


Fig. 10 Comparison of $\sim 1.54 \mu\text{m}$ PL intensities between Er^{3+} (5 mol %)- Yb^{3+} (10-50 mol %) and Er^{3+} (5 mol %)- Y^{3+} (10-50 mol %) codoped TiO_2 system annealed at 700 °C for 1 h.